



# Application of Statistical Learning Methods to a Data Set of Measured Heat Transfer Coefficients for Continuous Casting

Monika Seidl<sup>1,2</sup>, Daniel Kavić<sup>1,2</sup>, Sergiu Ilie<sup>3</sup>, and Christian Bernhard<sup>2</sup>

<sup>1</sup>K1-MET GmbH, Leoben, Austria

<sup>2</sup>Technical University of Leoben, Leoben, Austria

<sup>3</sup>Voestalpine Stahl GmbH, Linz, Austria

Received March 28, 2025; accepted April 3, 2025; published online May 26, 2025

**Abstract:** The heat transfer coefficient (HTC) between water and air/water sprays and the strand surface is a major parameter to simulate solidification in continuous casting processes. The HTC can be calculated via various equations from literature. However, based on in-house measurements, the application of statistical models for predicting local HTCs has become possible. Several models have been set up using Python coding and compared regarding the error metrics (root mean squared error and mean absolute error).

**Keywords:** Regression model, Heat transfer coefficient, Solidification, Simulation, Continuous casting, Spray cooling

**Anwendung statistischer Lernmethoden auf einen Datensatz gemessener Wärmeübergangskoeffizienten beim Stranggießen**

**Zusammenfassung:** Der Wärmeübergangskoeffizient (HTC) zwischen Wasser- und Luft/Wasser-Sprays und der Strangoberfläche ist ein wesentlicher Parameter zur Simulation der Erstarrung beim Stranggussverfahren. Der HTC kann über verschiedene Gleichungen aus der Literatur berechnet werden. Basierend auf eigenen Messungen wurde auch die statistische Vorhersage von lokalen HTCs möglich. Es wurden mehrere Modelle mittels Python-Programmierung erstellt und hinsichtlich der Fehlermetriken (Wurzel des mittleren quadratischen Fehlers und mittlerer absoluter Fehler) verglichen.

**Schlüsselwörter:** Regressionsmodell, Wärmeübergangskoeffizient, Erstarrung, Simulation, Strangguss, Sprühkühlung

## 1. Introduction

In continuous casting of steel, slab cooling plays a dominant role in controlling the process with respect to efficiency and product quality. Controlled cooling by spray water ("air-mist cooling") is a key to controlling the formation of surface and internal defects. Therefore, the length of secondary cooling is divided into cooling zones. The amount of water applied to the strand surface and the adjusted air pressure vary for each cooling zone and depend on the cast steel grade. These parameters are stored in so-called "cooling tables". For the whole product mix of a casting machine and the related casting parameters, a wide range of possible combinations of cooling parameters, and thus local heat transfer, exist. To predict solidification in a continuous casting process, on-line and off-line numerical simulation is today state-of-the-art. At the Chair of Ferrous Metallurgy at the Technical University of Leoben, an off-line simulation platform called "m<sup>2</sup>CAST" has been developed to use experimental measurement data in high resolution from the in-house nozzle measuring stand (NMS) as a thermal boundary condition. The collected data includes eleven parameters, among them the local water impact density (WID) from the water distribution (WD) measurement and the local heat transfer coefficient (HTC) for various operating parameters and nozzle types. To reduce the number of time-consuming measurements to a minimum, regression modelling was recently applied for the first time on the voluminous data sets providing a data-driven thermal boundary condition for solidification simulation [1, 2]; further results are presented in this contribution.

M. Seidl (✉)  
 Technical University of Leoben,  
 Franz-Josef-Straße 18,  
 8700 Leoben, Austria  
[monika.seidl@stud.unileoben.ac.at](mailto:monika.seidl@stud.unileoben.ac.at); [monika.seidl@k1-met.com](mailto:monika.seidl@k1-met.com)

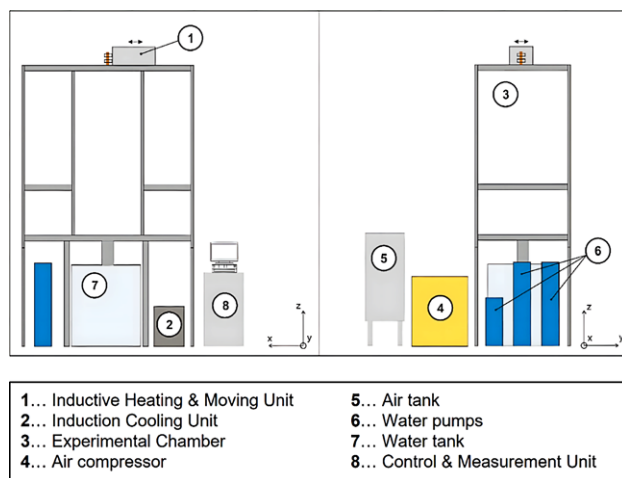


Fig. 1: Structure of the Nozzle Measuring Stand at Technical University of Leoben [3]

## 2. Nozzle Measuring Stand (NMS)

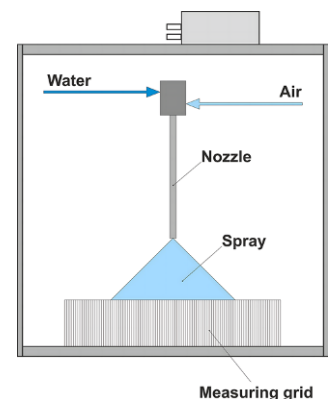
### 2.1 Structure

The nozzle measuring stand (NMS) was engineered to simulate the conditions of the secondary cooling zone *via* determining the local WID and the local HTC for various operating parameters and nozzle types. In Fig. 1 the schematic layout of its construction is presented. A special feature of the NMS is the possibility of installing two nozzles in a spatial arrangement, such as in a secondary cooling zone, thus measuring the spray overlap area. This leads to valuable additional information for certain spray parameters [1, 3].

### 2.2 Water Distribution (WD) Measurement

To measure the amount of water that impinges on the surface, the nozzles must be installed as shown in Fig. 2; [3]. For the measurement, seven parallelly arranged measuring grids are used, whereby the top view on the grids can be seen in Fig. 3b), together with a visualization of the dis-

Fig. 2: Schematic build of a water distribution measurement [3]



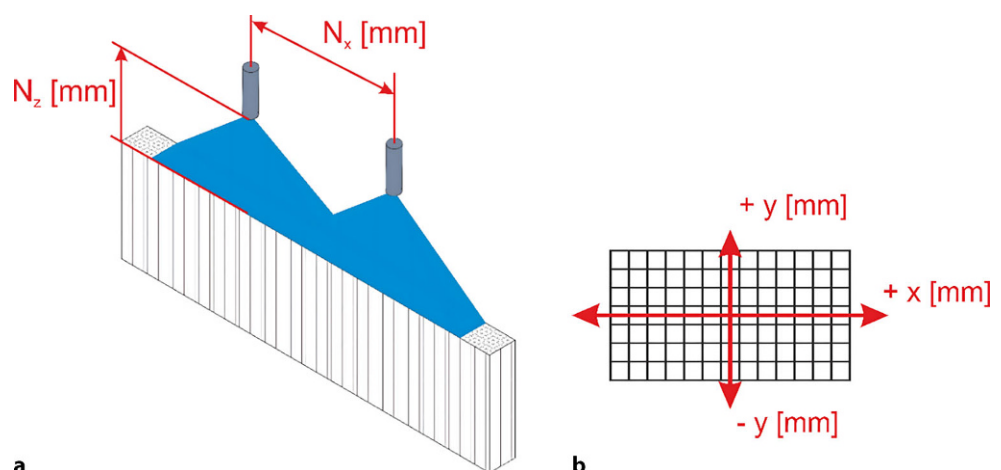
tance between the nozzle tips ( $N_x$ ) and the span between the nozzle tip and the surface ( $N_z$ ) under a) [3].

After a defined time under the water spray, the measuring grids are removed from the NMS and photographed separately. Using photo-optical analytics, the water distribution can be quantified and visualized (example given in Fig. 4). Furthermore, the WD in  $\text{lm}^{-2}$  is converted to the local water impact density (WID) in  $\text{kgm}^{-2}\text{s}^{-1}$  by using the time span.

### 2.3 Heat Transfer Coefficient (HTC) Measurement

For the measurement of the HTC, the nozzles must be rotated by  $180^\circ$  to spray the water at the ceiling, where the inductively heated and moveable specimen is located. The schematic structure is shown in Fig. 5a). The specimen itself is insulated to assume a one-dimensional heat conduction. The sample is heated up to a specific start temperature  $T_{\text{Start}}$  with the use of an inductive heating unit and is moved multiple times through the spray at different positions. The drop of the temperature is thereby measured via the three thermocouples. The schematic layout can be seen in Fig. 5b). The measurements are used to calculate the surface temperature and the HTC using an inverse heat conduction model [3].

Fig. 3: a Parameter  $N_x$  (distance between nozzle tips) and  $N_z$  (distance nozzle tip to surface), b visualization of the grid of the measuring chambers from above [3]



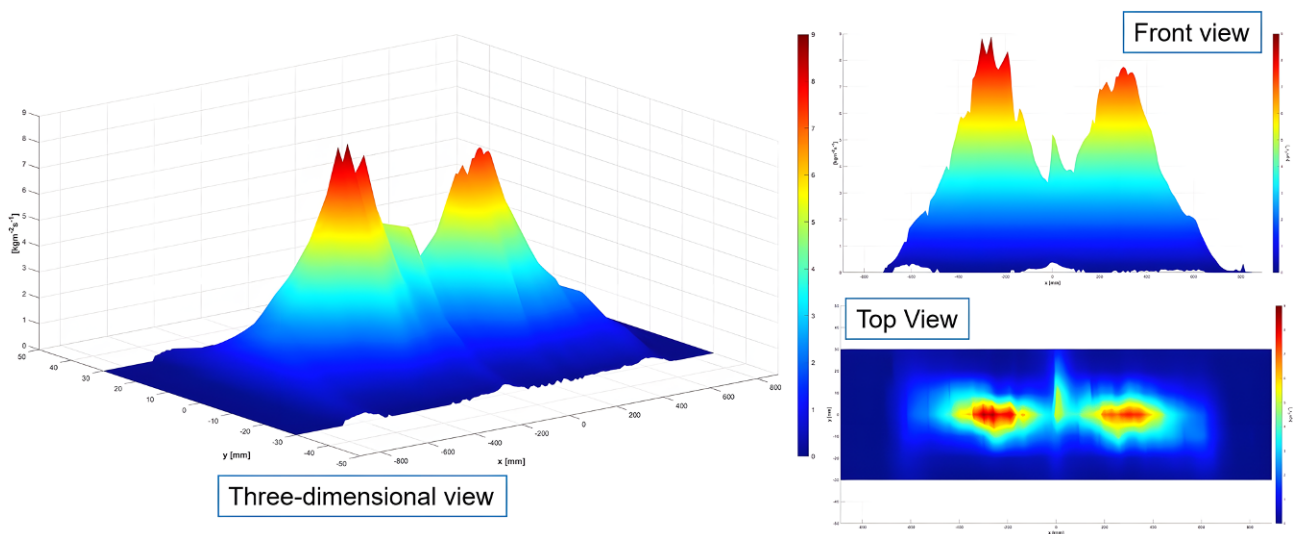
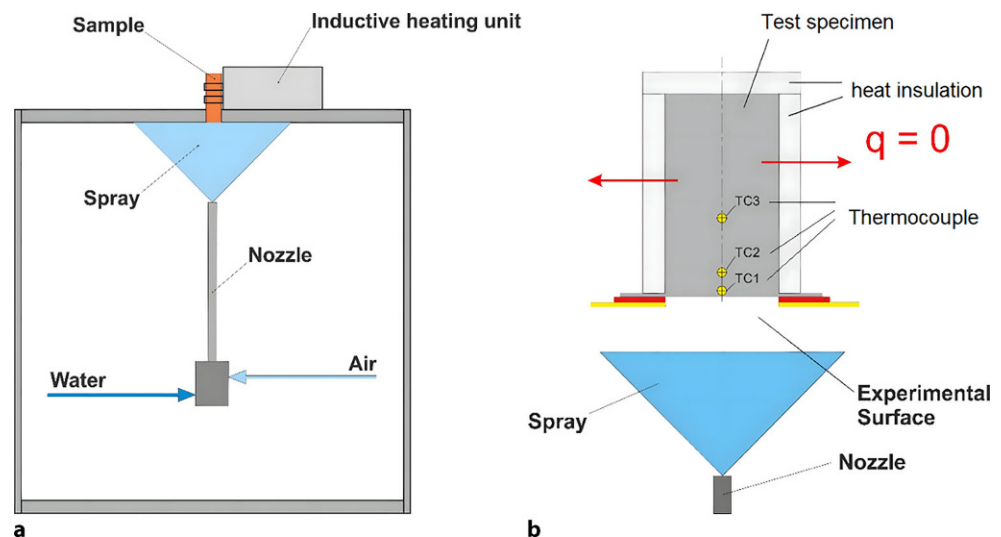


Fig. 4: Visualization of the water impact density in a 3D, a front and a top view

Fig. 5: **a** Scheme of measuring the heat transfer coefficient, **b** schematic structure of a specimen [3]



## 2.4 Data Triplets from Measurement

The measured WID is correlated to the calculated HTC and surface temperature  $T_s$ . With the involvement of the sample velocity, a specific HTC and  $T_s$  can be assigned to every chamber with the “x-position” and, therefore, its WID. Figure 6 gives a conception of this correlation. These data triples, together with the operating parameters, are used to parametrize regression models to predict the HTC, which will be explained in Sect. 2.6.

## 2.5 Simulation software m<sup>2</sup>CAST

The simulation platform m<sup>2</sup>CAST includes a solver for the 2D heat conduction and solidification problem, employing the two-dimensional finite volume method (FVM) coupled with the implicit alternating direction and inverse-enthalpy method, providing a CPU-time-saving solution in high-res-

olution. The heat transfer between the support rolls is divided into four zones as shown in Fig. 7. At the NMS, the HTC of zone III (spray cone) can be measured [1, 3–8].

- |      |                      |
|------|----------------------|
| I.   | Support rolls        |
| II.  | Pre-spray zone       |
| III. | Spray cone zone      |
| IV.  | Post-spray cone zone |
| V.   | Radiation            |

Currently, there are two different ways to define the HTC for the simulation. One possibility delivered Preuler [9] by investigating the HTC measurements and deriving an equation of a non-linear log-normal function to calculate the HTC depending on the WID and the surface temperature. The second option is based on the findings of Wendelsdorf et al. [10], who developed another empirical description of the phenomenon. However, modeling with regressions repre-

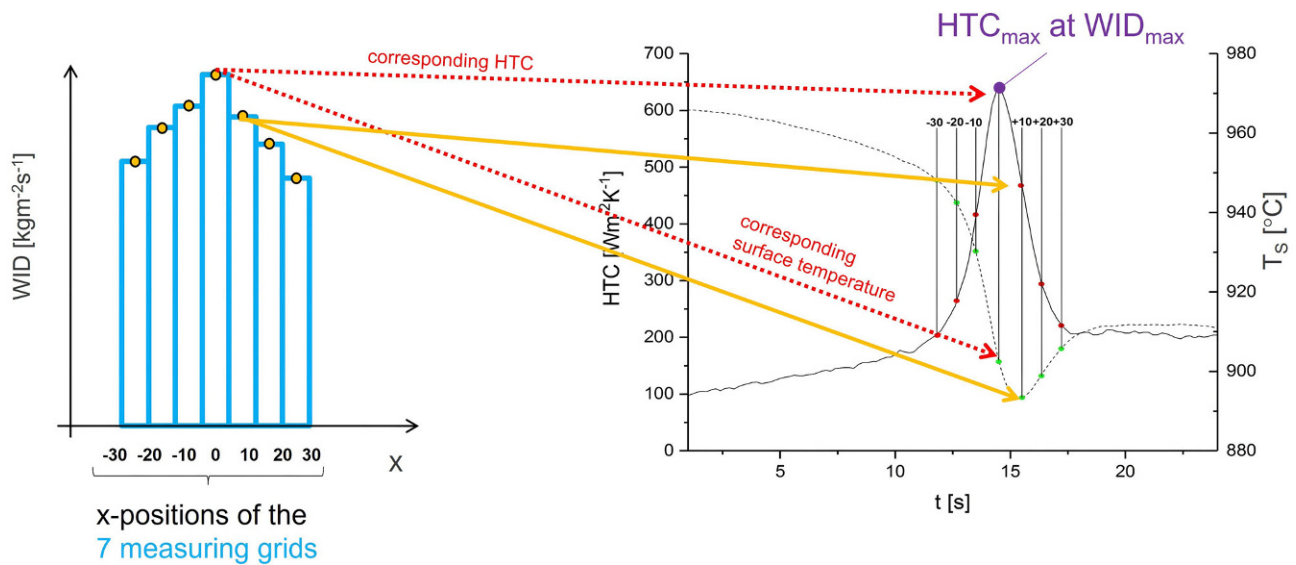


Fig. 6: Corresponding data triplets water impact density—heat transfer coefficient—surface temperature

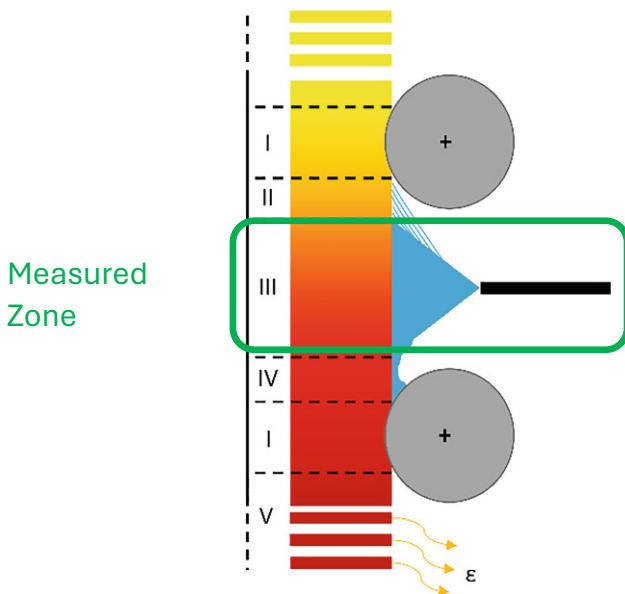


Fig. 7: Secondary cooling zones [8]

sents a new concept, which will be described further in the following section.

## 2.6 Prediction of the HTC Using Regression Models

The statistical regression approach is employed to predict variables of interest based on extensive datasets of independent variables, without explicitly defining the underlying functional dependencies or physicochemical relationships, thereby representing a “black-box” modeling paradigm. This methodology relies on the acquisition and analysis of large-scale data to establish empirical correlations between target variables and relevant process

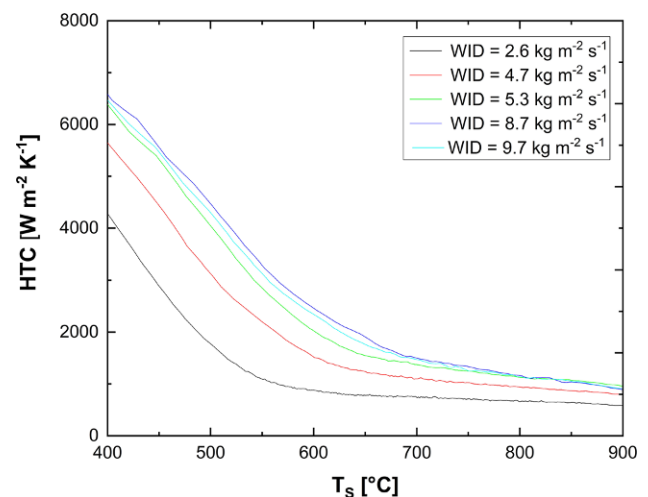


Fig. 8: Course of the HTC against  $T_s$  in dependency of the WID [9]

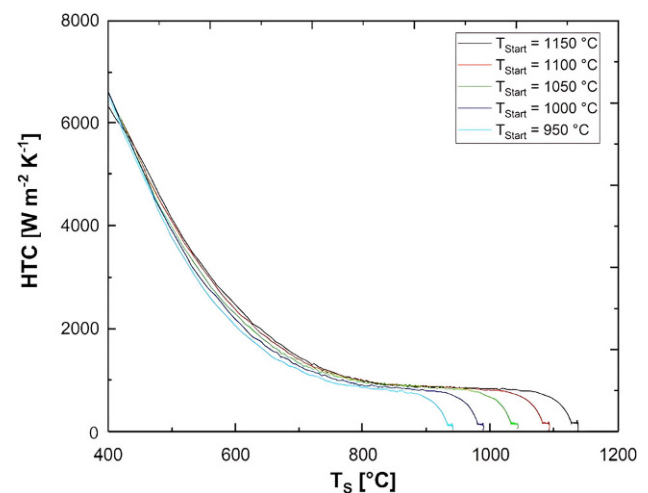


Fig. 9: Course of the HTC against  $T_s$  in dependency to  $T_{Start}$  [9]

TABLE 1  
Collection of rounded value ranges for the parameters of the dataset

Parameter	Unit	Range
$T_{\text{Start}}$	°C	950–1195
$N_x$	mm	0–801
$N_z$	mm	130–310
$V_{\text{H}_2\text{O}}$	$\text{l min}^{-1}$	1.45–17
$p_{\text{H}_2\text{O}}$	bar	0.8–9.4
$p_{\text{Air}}$	bar	0–2.7
$v$	$\text{m min}^{-1}$	0.7–1.9
$x_{\text{Pos}}$	mm	0–700
$T_s$	°C	729.58–1142.64
WID	$\text{kg m}^{-2} \text{s}^{-1}$	0–55

features, enabling data-driven insights without requiring prior mechanistic knowledge. In the case of the HTC, there is a study on this topic by Taferner et al. [1, 2]. For the following prediction, these parameters have been used:

- $N_z$ : distance nozzle to surface
- $x_{\text{Pos}}$ : x-position in spray width
- $V_{\text{H}_2\text{O}}$ : water flow rate
- $p_{\text{H}_2\text{O}}$ : water pressure
- $p_{\text{Air}}$ : air pressure
- $T_s$ : surface temperature
- WID: water impact density

In the first work of Taferner et al. [1], the commercial software package MATLAB was used to create different regression models, whereby an exponential gaussian regression model delivered the best results.

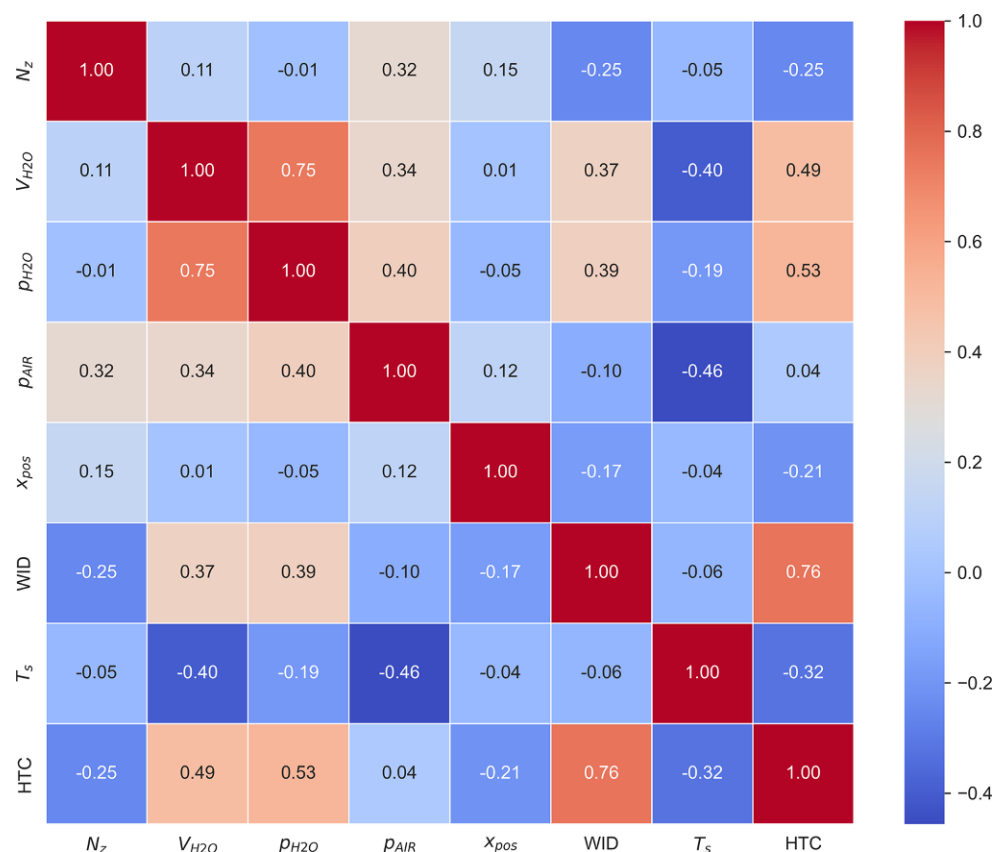
### 3. Results & Discussion

#### 3.1 Description of the Dataset

For the statistical investigation, nozzles and spraying parameters for a wide variety of cooling tables of a casting machine at voestalpine Stahl GmbH in Linz were utilized for the WID and HTC measurement at the NMS. All the statistical learning models were developed using Python (Version 3.12.3). Additionally, the following packages have been used: Pandas (2.2.2), NumPy (1.26.4), Scikit-Learn (1.6.0), Matplotlib (3.8.4), Plotly (5.22.0), and Seaborn (0.13.2).

In the beginning some data cleansing steps were applied. Firstly, high values distorted by the “Leidenfrost-Effect” have been removed from the initial dataset. To set the range of the useable data, the lower limit for the surface temperature was chosen to be 700 °C. This specific value can be explained by looking at Fig. 8 from so-called “boiling curves” [9]. For this specific kind of measurement, the specimen is kept in a local position within the spray with a predefined initial temperature. The measured HTCs accord to a constant WID and just depend on  $T_s$ . This provides the definition of the Leidenfrost temperature for the chosen

Fig. 10: Pearson correlation matrix



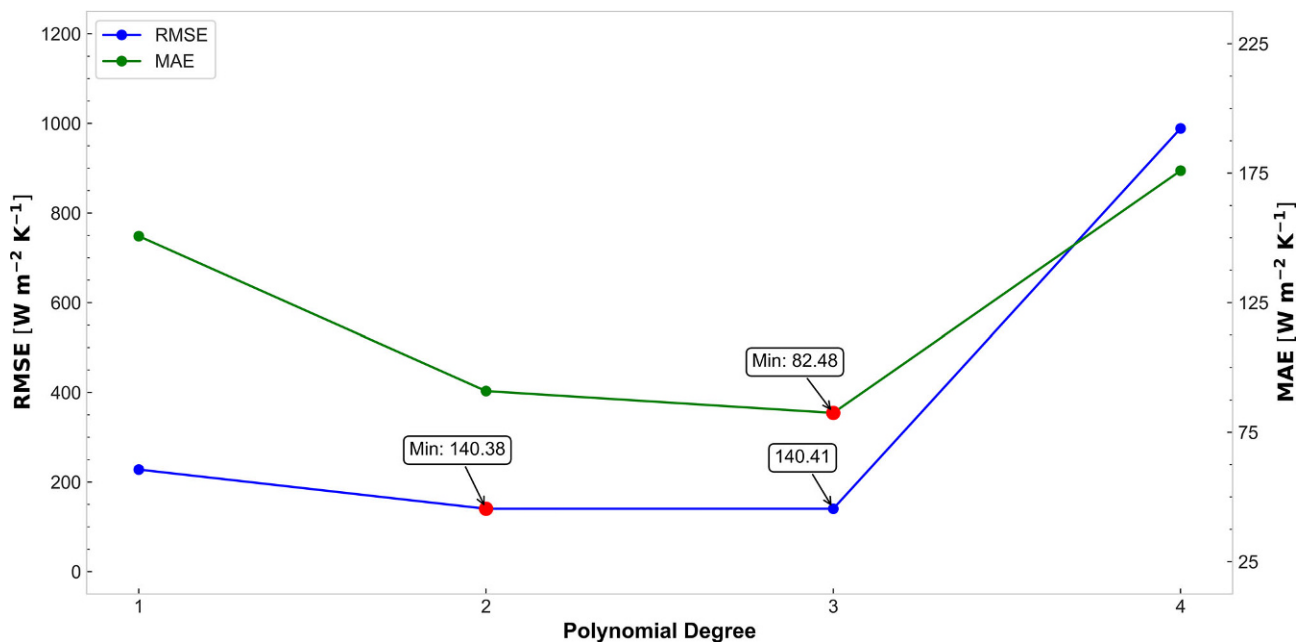


Fig. 11: RSME and MAE against polynomial degree for a polynomial regression model

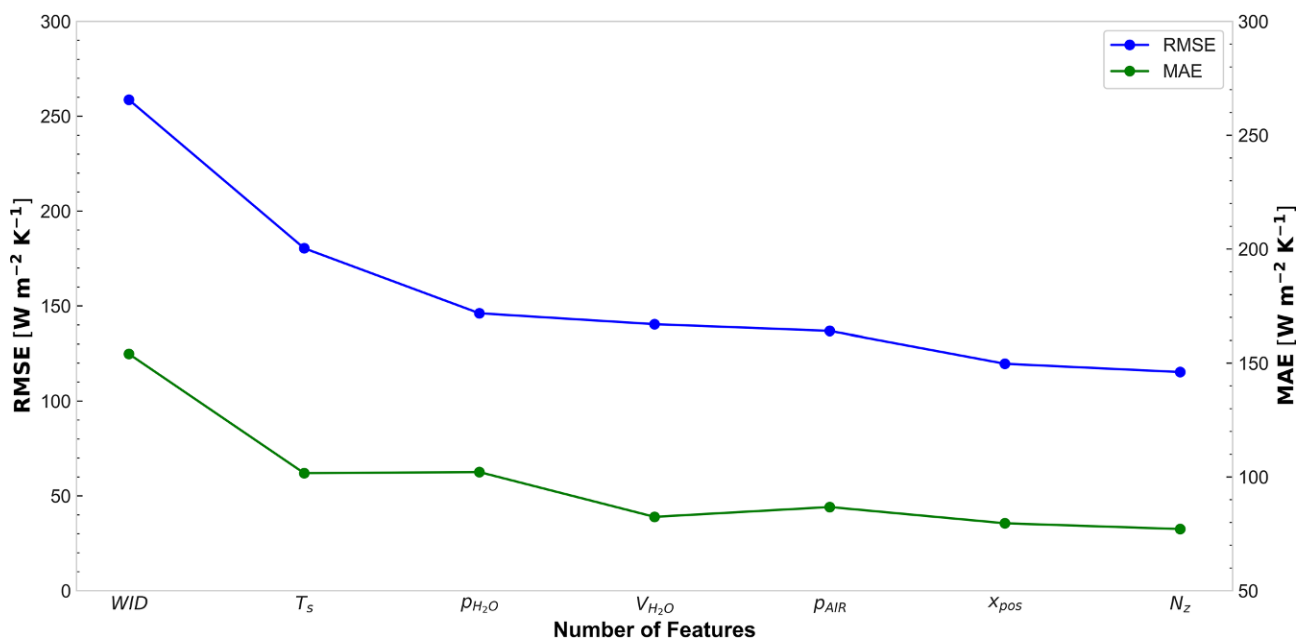


Fig. 12: RSME and MAE against number of features for a polynomial regression model

experimental setup. In the temperature range of stable film vaporization, the HTC shows only a moderate dependency from  $T_s$ , even if influenced by WID. When coming closer to the Leidenfrost temperature, which, as expected, also depends on WID, the HTC increases significantly. As the physics of heat transfer changes when the temperature falls below Leidenfrost, 700°C was chosen as the lower threshold of  $T_s$  for simplicity.

Preuler investigated also the influence of the starting temperature  $T_{Start}$  as shown in Fig. 9. Within the first seconds of measurement, the capacitive heating of the

measurement device lowers the recalculated HTC. For the present work, a  $T_s$  of 50 °C below  $T_{Start}$  was assumed as the upper threshold.

After data cleansing, a total of 1892 datasets remain for the analysis. From this final data set, 129 observations correspond to single-fluid-nozzles and the remaining amount to twin-fluid-nozzles. In Table 1, all parameters including their units and ranges are listed.

Using the final data set, a train-test split in a randomized fashion with a ratio of  $\frac{3}{4}$  to  $\frac{1}{4}$  was conducted and used for



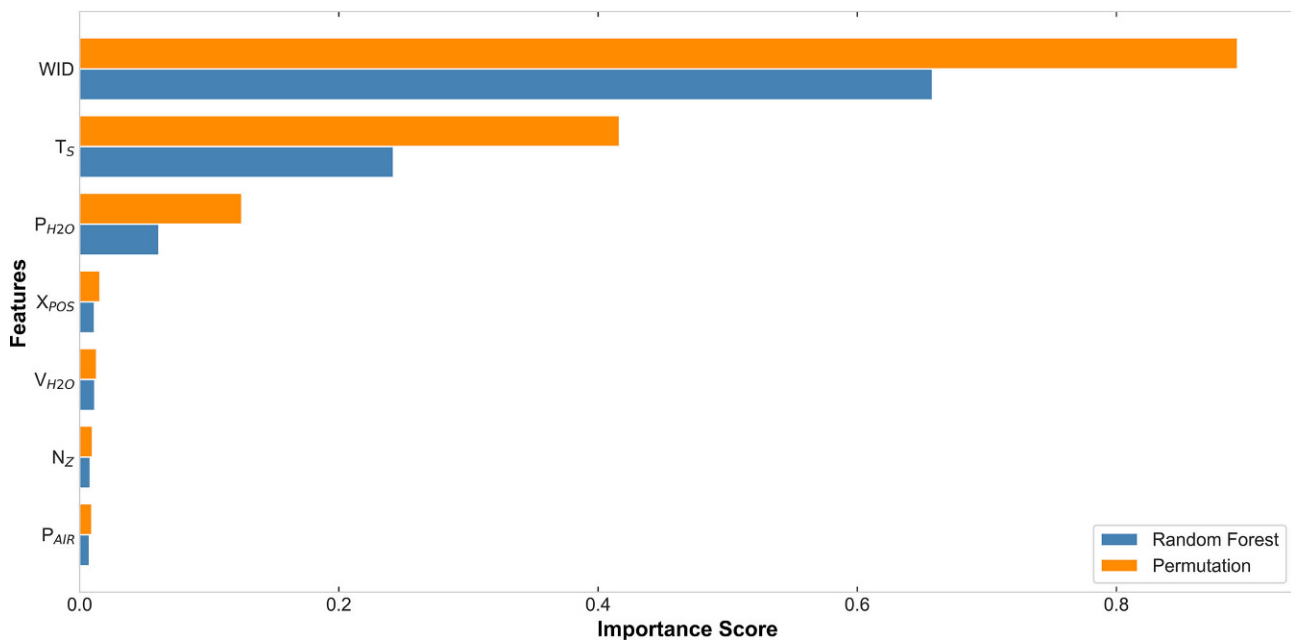


Fig. 13: Random forest and permutation feature importance for a random forest regression model

all six regression models. This guarantees a non-biased training of the models.

### 3.2 Study of Parameters

As described in Sect. 2.6, Taferner et al. [1] used ten parameters for the developed regression models. Anyhow, a lower number of used features could prevent overfitting and increase the quality of the prediction. Hence, an investigation on the statistical relevance of the spray parameters has been conducted.

A Pearson correlation matrix was generated using the complete data set shown in Fig. 10. Focusing on the last row, the results indicate that the WID with a value of 0.76 has the strongest positive linear correlation. On the other hand, the analysis pointed out that  $T_s$  has, with a factor of  $-0.32$ , a substantial negative influence on the HTC. Another important parameter with a positive correlation would be the water pressure and flow rate, whereas the air pressure  $p_{AIR}$  shows a neglectable influence. The parameter  $N_z$  symbolizes the impingement angle of the spray droplets at the surface and also seems to have only a moderate influence.

Considering that the Pearson correlation matrix only shows a linear correlation between two parameters, additional methods to investigate the impact of independent features on the variable of interest, like variable importance using the Random Forest algorithm or a feed-forward selection approach during polynomial regression, have been applied.

### 3.3 Regression Models

A comprehensive investigation was carried out using six different regression models and the prepared data set. In the following sections, the applied regression models and their selected model parameters are discussed in detail, except for the linear regression, as there are no adjustable model properties. It should be mentioned that the models were initially trained and tested using all the parameters outlined in Sect. 2.6. Additionally, they were also evaluated using only WID and  $T_s$  as the prediction parameters. Figure 14 provides an overview of the error metrics root mean squared error (RSME) and mean absolute error (MAE) for all models.

#### 3.3.1 Polynomial Regression (PR) Model

Regarding the choice of the polynomial degree, Fig. 11 shows that both error criteria (RMSE and MAE) do not have their lowest values at the same degree. However, the RSME for a 2nd and 3rd degree is approximately the same. Therefore, the latter degree was used for modeling.

Furthermore, the results of the feed forward selection are visible in Fig. 12. It shows the decreasing error values against the number of selected features, with the first selected parameter being the most important, the second one the second most important, and so on. The outcome of the analysis is that the error drops the most if  $T_s$  was further more used to the WID as a feature. Additional parameters contribute to a decrease of the error criteria, however, not significantly.

### 3.3.2 Random Forest Regression (RFR) Model

This regression model employs an ensemble learning approach. The model is constructed using 100 decision trees. The model undergoes a 5-fold cross-validation. All other settings remain at their default values.

For this model a “feature importance” (based on tree splits) and “permutation feature importance” (based on model performance drop) have been performed. As it can be seen in Fig. 13, the same two parameters ( $WID$  and  $T_S$ ) deliver the highest influence on the model’s accuracy, again followed by the water pressure  $p_{H_2O}$ .

### 3.3.3 Gradient Boosting Regression (GBR) Model

The gradient boosting regression model uses 200 decision trees, each correcting the residual errors of the combined prediction from all previous trees. Additionally, the data is standardized, and the model uses a learning rate of 0.1 with a maximum tree depth of 5, balancing bias and variance.

### 3.3.4 Support Vector Regression (SVR) Model

This model utilizes an RBF kernel. It applies Min-Max scaling to both features and target values for improved numerical stability. Hyperparameter tuning is performed using a RandomizedSearchCV together with a 5-fold cross-validation to optimize C, gamma, and epsilon.

### 3.3.5 Gaussian Process Regression (GPR) Model

For this model, a radial basis function (RBF) kernel combined with a WhiteKernel is used. Additionally, a hyperparameter optimization with 10 restarts are added. Standardization is applied as well.

## 3.4 Comparison of the Models

Several different regression models were established and compared to each other. Figure 14 shows the RSME and

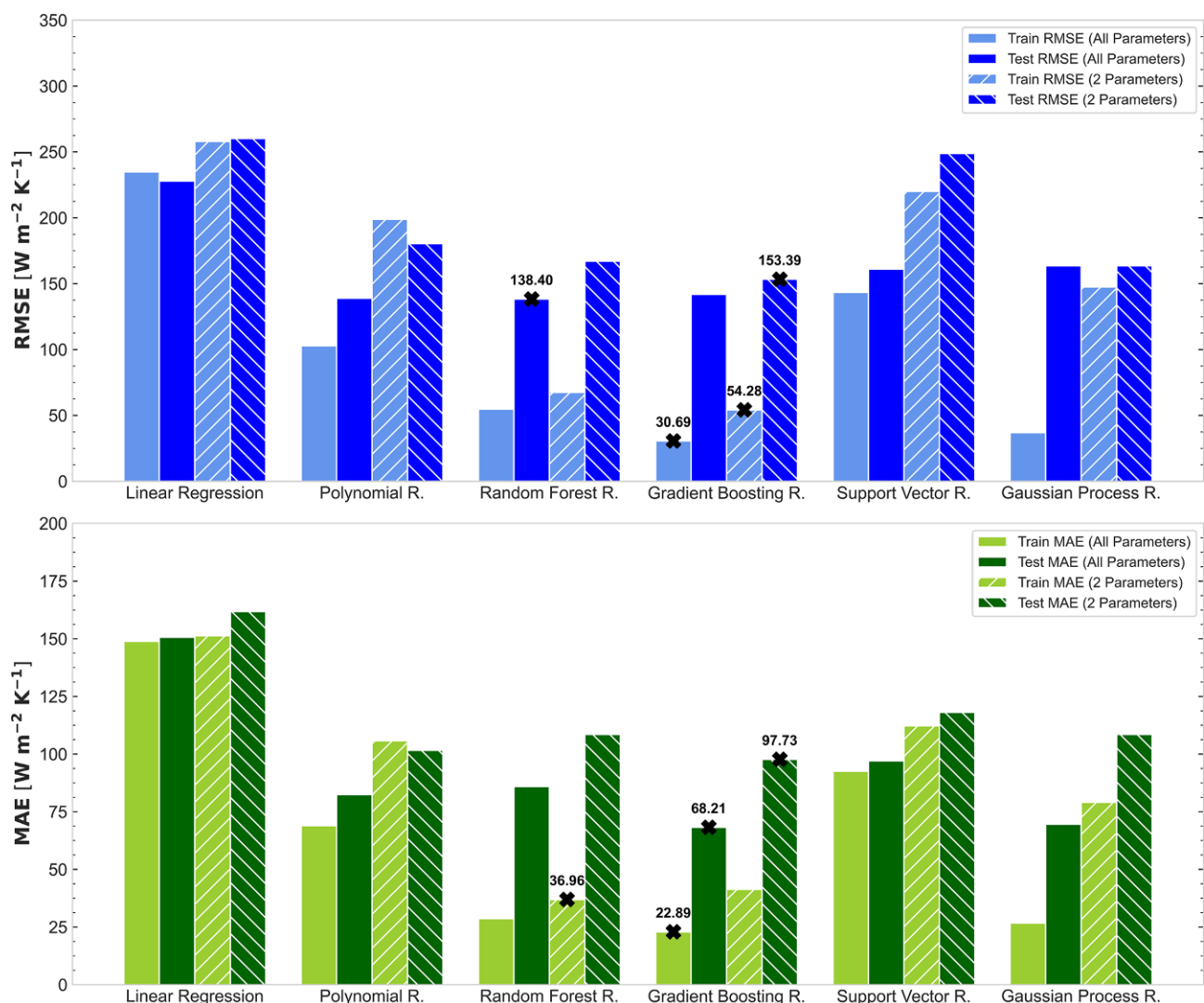


Fig. 14: Comparison of the error values (RSME and MAE) for all six regression models for the training and test set



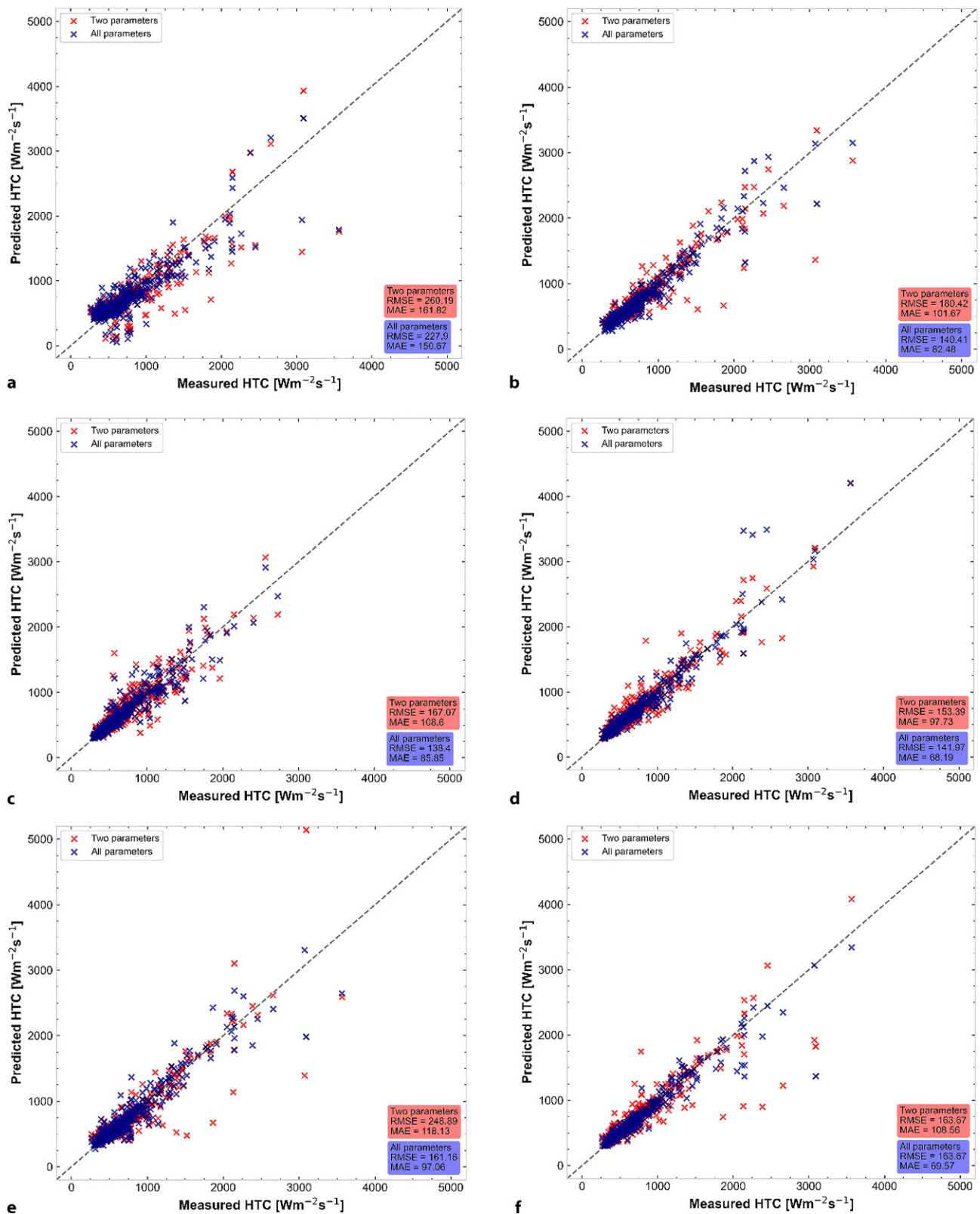


Fig. 15: Regression Models with the usage of all (purple) or only two parameters (red) for **a** Linear Regression, **b** Polynomial Regression, **c** Random Forest Regression, **d** Gradient Boosting Regression, **e** Support Vector Regression, **f** Gaussian Process Regression

MAE values for the training and test set of all applied models. It can be observed that a linear regression yields to the highest error values. This confirms that a Pearson correlation matrix alone cannot give enough information about the variable dependencies. The best MAE for the testing set was found for the GBR with the usage of all parameters. This model also led to the lowest RMSE value for the training set, considering only WID and  $T_s$ . Overall, this model delivered the best performance. Furthermore, it can be observed that the error values increase when just two parameters are used. The magnitude of this difference depends on the selected model. For the GBR, the RFR, and the SVR model, the increase is not significantly high. In contrast, it has a greater impact on the GPR and PR. In Fig. 15 all plots of the predicted versus the calculated HTC for the test sets are given.

## 4. Conclusion

This contribution uses data-driven methods to predict the HTC in the spray cone region as a function of different nozzle parameters and slab surface temperatures. Comprehensive data cleansing processes were performed to provide a high-quality data set for modeling. The relationship between the independent features and the target variable was then analyzed using various statistical methods.

Six different statistical methods were applied for modeling. Among these, GPR achieved the best results in terms of RMSE and MAE on the test dataset.

The analysis of the variable importance and the modeling results clarified that the WID and  $T_s$ , in particular, have the greatest influence on the HTC.

**Acknowledgements.** The authors gratefully acknowledge the funding support of K1-MET GmbH, metallurgical competence center. The research program of the K1-MET competence center is supported by COMET (Competence Center for Excellent Technologies), the Austrian program for competence centers. COMET is funded by the Federal Ministry for Climate Action, Environment, Energy, Mobility, Innovation and Technology, the Federal Ministry for Labour and Economy, the Federal States of Upper Austria, Tyrol and Styria as well as the Styrian Business Promotion Agency (SFG) and the Standortagentur Tyrol. Furthermore, Upper Austrian Research GmbH continuously supports K1-MET. Beside the public funding from COMET, this research project is partially financed by the Montanuniversität Leoben and the industrial partners voestalpine Stahl Linz GmbH and Ternium Brazil.

**Funding.** Open access funding provided by Montanuniversität Leoben.

**Open Access** Dieser Artikel wird unter der Creative Commons Namen-

snennung 4.0 International Lizenz veröffentlicht, welche die Nutzung, Vervielfältigung, Bearbeitung, Verbreitung und Wiedergabe in jeglichem Medium und Format erlaubt, sofern Sie den/die ursprünglichen Autor(en) und die Quelle ordnungsgemäß nennen, einen Link zur Creative Commons Lizenz beifügen und angeben, ob Änderungen vorgenommen wurden. Die in diesem Artikel enthaltenen Bilder und sonstiges Drittmaterial unterliegen ebenfalls der genannten Creative Commons Lizenz, sofern sich aus der Abbildungslegende nichts anderes ergibt. Sofern das betreffende Material nicht unter der genannten Creative Commons Lizenz steht und die betreffende Handlung nicht nach gesetzlichen Vorschriften erlaubt ist, ist für die oben aufgeführten Weiterverwendungen des Materials die Einwilligung des jeweiligen Rechteinhabers einzuholen. Weitere Details zur Lizenz entnehmen Sie bitte der Lizenzinformation auf <http://creativecommons.org/licenses/by/4.0/deed.de>.

## References

1. Taferner, M., Laschinger, J., Bernhard, C., Bernhard, M., Ilie, S.: Effect of nozzle parameters on the cooling conditions in the secondary cooling zone of a slab caster. BHM Berg- und Hüttenmännische Monatshefte (2023). <https://doi.org/10.1007/s00501-023-01402-y>
2. Taferner, M.: Vorhersage des lokalen Wärmeübergangs im Stanggießprozess durch Laborversuche und Regressionsmodelle. Montanuniversität Leoben, Leoben (2024)
3. Preuler, L., Bernhard, C., Ilie, S., Six, J.: Experimental investigations on spray characteristics of water-air nozzles. BHM Berg- und Hüttenmännische Monatshefte (2018). <https://doi.org/10.1007/s00501-017-0693-5>
4. A 2D—finite volume solidification software for real-time simulation of continuous slab casting. In: Kavić, D., Bernhard, M., Wieser, G., Taferner, M., Ilie, S., Bernhard, C. (eds.) 11th European continuous casting conference ECC. Essen (2024)
5. Michelis, S., Bernhard, C., Rauter, W., Erker, M., Sorman, A.: Modelling solidification in continuous casting: algorithms and boundary conditions (2009)
6. Development, implementation and verification of a transient numeric solidification model of a continuous bloom caster at Voestalpine Stahl Donawitz. In: Michelis, S., Bernhard, C., Rauter, W., Erker, M., Brandl, W., Reiter, J., Sorman, A. (eds.) 7th European continuous casting conference. Düsseldorf, Germany (2011)
7. Bernhard, M., Santos, G., Preuler, L., Taferner, M., Wieser, G., Laschinger, J., Ilie, S., Bernhard, C.: A near-process 2D heat-transfer model for continuous slab casting of steel. Steel Res. Int. (2022). <https://doi.org/10.1002/srin.202200089>
8. Kavić, D.: Entwicklung eines 2D Erstarrungsmodells für das Stranggießen von Stahl. Montanuniversität Leoben, Leoben (2023)
9. Preuler, L.: Charakterisierung der Spritzwasserkühlung in der Sekundärkühlzone einer Brammenstranggießanlage. Montanuniversität Leoben, Leoben (2019)
10. Wendelstorf, R., Spitzer, K.-H., Wendelstorf, J.: Effect of oxide layers on spray water cooling heat transfer at high surface temperatures. International Journal of Heat and Mass Transfer (2008). <https://doi.org/10.1016/j.ijheatmasstransfer.2008.01.033>

**Publisher's Note.** Springer Nature remains neutral with regard to jurisdictional claims in published maps and institutional affiliations.